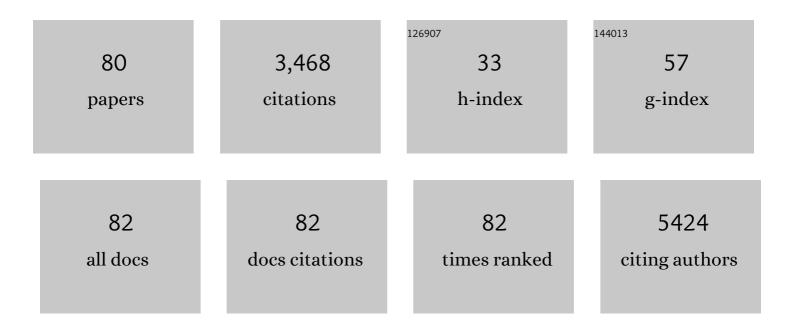


List of Publications by Year in descending order

Source: https://exaly.com/author-pdf/3591439/publications.pdf Version: 2024-02-01



YAN MI

#	Article	IF	CITATIONS
1	Large-scale highly ordered Sb nanorod array anodes with high capacity and rate capability for sodium-ion batteries. Energy and Environmental Science, 2015, 8, 2954-2962.	30.8	294
2	Fe(III) modified BiOCl ultrathin nanosheet towards high-efficient visible-light photocatalyst. Nano Energy, 2016, 30, 109-117.	16.0	185
3	Enhancement of Sodium Ion Battery Performance Enabled by Oxygen Vacancies. Angewandte Chemie - International Edition, 2015, 54, 8768-8771.	13.8	180
4	Multiple nanostructures based on anodized aluminium oxide templates. Nature Nanotechnology, 2017, 12, 244-250.	31.5	168
5	Highly Ordered Three-Dimensional Ni-TiO ₂ Nanoarrays as Sodium Ion Battery Anodes. Chemistry of Materials, 2015, 27, 4274-4280.	6.7	140
6	Constructing a AZO/TiO ₂ Core/Shell Nanocone Array with Uniformly Dispersed Au NPs for Enhancing Photoelectrochemical Water Splitting. Advanced Energy Materials, 2016, 6, 1501496.	19.5	129
7	p-Type CuBi ₂ O ₄ : an easily accessible photocathodic material for high-efficiency water splitting. Journal of Materials Chemistry A, 2016, 4, 8995-9001.	10.3	124
8	Manipulation of charge transfer and transport in plasmonic-ferroelectric hybrids for photoelectrochemical applications. Nature Communications, 2016, 7, 10348.	12.8	113
9	Switchable Chargeâ€Transfer in the Photoelectrochemical Energy onversion Process of Ferroelectric BiFeO ₃ Photoelectrodes. Angewandte Chemie - International Edition, 2014, 53, 11027-11031.	13.8	106
10	Stereoselective Solid‣tate Synthesis of Substituted Cyclobutanes Assisted by Pseudorotaxaneâ€like MOFs. Angewandte Chemie - International Edition, 2018, 57, 12696-12701.	13.8	103
11	Designing Heterogeneous 1D Nanostructure Arrays Based on AAO Templates for Energy Applications. Small, 2015, 11, 3408-3428.	10.0	92
12	Coordination-Driven Stereospecific Control Strategy for Pure Cycloisomers in Solid-State Diene Photocycloaddition. Journal of the American Chemical Society, 2020, 142, 700-704.	13.7	90
13	2D CoOOH Sheet-Encapsulated Ni2P into Tubular Arrays Realizing 1000ÂmAÂcmâ^'2-Level-Current-Density Hydrogen Evolution Over 100Âh in Neutral Water. Nano-Micro Letters, 2020, 12, 140.	27.0	83
14	Highly Controllable Surface Plasmon Resonance Property by Heights of Ordered Nanoparticle Arrays Fabricated <i>via</i> a Nonlithographic Route. ACS Nano, 2015, 9, 4583-4590.	14.6	74
15	Costâ€effective Atomic Layer Deposition Synthesis of Pt Nanotube Arrays: Application for High Performance Supercapacitor. Small, 2014, 10, 3162-3168.	10.0	71
16	Building of anti-restack 3D BiOCl hierarchitecture by ultrathin nanosheets towards enhanced photocatalytic activity. Applied Catalysis B: Environmental, 2015, 176-177, 331-337.	20.2	69
17	Single-metal-atom catalysts: An emerging platform for electrocatalytic oxygen reduction. Chemical Engineering Journal, 2021, 406, 127135.	12.7	67
18	Nanoengineering Energy Conversion and Storage Devices via Atomic Layer Deposition. Advanced Energy Materials, 2016, 6, 1600468.	19.5	63

#	Article	IF	CITATIONS
19	Fabrication of ultrathin single-layer 2D metal–organic framework nanosheets with excellent adsorption performance <i>via</i> a facile exfoliation approach. Journal of Materials Chemistry A, 2021, 9, 546-555.	10.3	55
20	A highly efficient visible-light driven photocatalyst: two dimensional square-like bismuth oxyiodine nanosheets. Dalton Transactions, 2014, 43, 9549-9556.	3.3	54
21	Amperometric Hydrogen Peroxide Biosensor Based on Horseradish Peroxidase Immobilized on Fe ₃ O ₄ /Chitosan Modified Glassy Carbon Electrode. Electroanalysis, 2009, 21, 1514-1520.	2.9	52
22	Understanding the Orderliness of Atomic Arrangement toward Enhanced Sodium Storage. Advanced Energy Materials, 2016, 6, 1600448.	19.5	52
23	Three-Dimensional Plasmonic Nanostructure Design for Boosting Photoelectrochemical Activity. ACS Nano, 2017, 11, 7382-7389.	14.6	48
24	Study of nimesulide and its determination using multiwalled carbon nanotubes modified glassy carbon electrodes. Electrochimica Acta, 2010, 55, 2522-2526.	5.2	46
25	Amperometric Hydrogen Peroxide Biosensor Based on Immobilization of Hemoglobin on a Glassy Carbon Electrode Modified with Fe3O4/Chitosan Core-Shell Microspheres. Sensors, 2009, 9, 6185-6199.	3.8	44
26	A photoelectrochemical aptasensor for the sensitive detection of streptomycin based on a TiO2/BiOI/BiOBr heterostructure. Analytica Chimica Acta, 2020, 1115, 33-40.	5.4	44
27	A pyrazolopyrimidine based fluorescent probe for the detection of Cu2+ and Ni2+ and its application in living cells. Spectrochimica Acta - Part A: Molecular and Biomolecular Spectroscopy, 2019, 209, 141-149.	3.9	43
28	Ultra-low mass loading of platinum nanoparticles on bacterial cellulose derived carbon nanofibers for efficient hydrogen evolution. Catalysis Today, 2016, 262, 141-145.	4.4	42
29	Template-Guided Programmable Janus Heteronanostructure Arrays for Efficient Plasmonic Photocatalysis. Nano Letters, 2018, 18, 4914-4921.	9.1	42
30	Room-Temperature Synthesis and Luminescent Properties of Single-Crystalline SrMoO4 Nanoplates. Journal of Physical Chemistry C, 2009, 113, 20795-20799.	3.1	37
31	Structure diversities of ten entangled coordination polymers assembled from reactions of Co(ii) or Ni(ii) salts with 5-(pyridin-4-yl)isophthalic acid in the absence or presence of auxiliary N-donor ligands. CrystEngComm, 2013, 15, 9553.	2.6	36
32	Facile surface treatment on Cu2O photocathodes for enhancing the photoelectrochemical response. Applied Catalysis B: Environmental, 2016, 198, 398-403.	20.2	36
33	Fully understanding the positive roles of plasmonic nanoparticles in ameliorating the efficiency of organic solar cells. Nanoscale, 2015, 7, 15251-15257.	5.6	34
34	Controllable multiple-step configuration transformations in a thermal/photoinduced reaction. Nature Communications, 2022, 13, .	12.8	32
35	In-situ surface-derivation of Ni-Mo bimetal sulfides nanosheets on Co3O4 nanoarrays as an advanced overall water splitting electrocatalyst in alkaline solution. Journal of Alloys and Compounds, 2019, 791, 328-335.	5.5	27
36	Single MoTe2 sheet electrocatalytic microdevice for in situ revealing the activated basal plane sites by vacancies engineering. Nano Research, 2021, 14, 4814-4821.	10.4	27

#	Article	IF	CITATIONS
37	Nitrogen-doped hollow porous carbon nanotubes for high-sulfur loading Li–S batteries. Electrochimica Acta, 2019, 324, 134849.	5.2	26
38	MOF-assisted three-dimensional TiO2@C core/shell nanobelt arrays as superior sodium ion battery anodes. Journal of Alloys and Compounds, 2018, 769, 257-263.	5.5	25
39	Second ligands-assisted structural variation of entangled coordination polymers with polycatenated or polythreaded features. CrystEngComm, 2013, 15, 1068-1076.	2.6	24
40	Nanovilli electrode boosts hydrogen evolution: A surface with superaerophobicity and superhydrophilicity. Nano Research, 2021, 14, 961-968.	10.4	24
41	Abnormal behaviors in electrical transport properties of cobalt-doped tin oxide thin films. Journal of Materials Chemistry, 2012, 22, 16060.	6.7	22
42	Dual-response detection of Ni ²⁺ and Cu ²⁺ ions by a pyrazolopyrimidine-based fluorescent sensor and the application of this sensor in bioimaging. RSC Advances, 2019, 9, 35671-35676.	3.6	21
43	Room temperature reverse-microemulsion synthesis and photoluminescence properties of uniform BaMoO4 submicro-octahedra. Materials Letters, 2009, 63, 742-744.	2.6	20
44	Enhanced photoelectrochemical performance of LaFeO ₃ photocathode with Au buffer layer. RSC Advances, 2019, 9, 26780-26786.	3.6	19
45	Unusual enhancement in electrical conductivity of tin oxide thin films with zinc doping. Physical Chemistry Chemical Physics, 2011, 13, 5760.	2.8	18
46	Engineering inner-porous cobalt phosphide nanowire based on controllable phosphating for efficient hydrogen evolution in both acidic and alkaline conditions. Applied Surface Science, 2019, 481, 1524-1531.	6.1	18
47	Oxygen vacancies and Bi2S3 nanoparticles co-sensitized TiO2 nanotube arrays for enhanced photoelectrochemical sensing of chlorpyrifos. Journal of Electroanalytical Chemistry, 2022, 911, 116220.	3.8	18
48	Gold nanochestnut arrays as ultra-sensitive SERS substrate for detecting trace pesticide residue. Nanotechnology, 2018, 29, 295502.	2.6	17
49	Stereoselective Solid‣tate Synthesis of Substituted Cyclobutanes Assisted by Pseudorotaxaneâ€like MOFs. Angewandte Chemie, 2018, 130, 12878-12883.	2.0	17
50	Ln-incorporated coordination complexes as fluorescence sensor for selective detection nitroaromatic compounds. Materials Chemistry and Physics, 2019, 232, 152-159.	4.0	17
51	Oxygen Deficient TiO2â^'x with Dual Reaction Sites for Activation of H2O2 to Degrade Organic Pollutants. Catalysis Letters, 2020, 150, 222-233.	2.6	17
52	Synthesis, structure, and properties of dinuclear copper (II) complex with a (H2O)12 cluster. Inorganic Chemistry Communication, 2009, 12, 628-631.	3.9	16
53	Growth control of AgTCNQ nanowire arrays by using a template-assisted electro-deposition method. Journal of Materials Chemistry C, 2013, 1, 8003.	5.5	16
54	Synthesis, characterization and luminescence properties of Eu(III) and Tb(III) complexes with novel pyrazole derivatives and 1,10-phenanthroline. Spectrochimica Acta - Part A: Molecular and Biomolecular Spectroscopy, 2010, 75, 825-829.	3.9	15

#	Article	IF	CITATIONS
55	A pillar-layer strategy to construct 2D polycatenated coordination polymers for luminescence detection of Cr ₂ O ₇ ^{2â^²} and CrO ₄ ^{2â^²} in aqueous solution. CrystEngComm, 2019, 21, 4943-4950.	2.6	15
56	Ultrathin BiOCl nanosheet modified TiO ₂ for the photoelectrochemical sensing of chlorpyrifos. Analytical Methods, 2019, 11, 375-380.	2.7	15
57	Tuning the configuration of the flexible metal–alkene-framework affords pure cycloisomers in solid state photodimerization. Chemical Communications, 2021, 57, 1129-1132.	4.1	13
58	Synthesis, structure, and properties of two novel copper(II) complexes, [Cu(phen)(L)2]·6H2O and [Cu(phen)3]·(ClO4)2. Inorganic Chemistry Communication, 2009, 12, 1189-1192.	3.9	12
59	Crystal structure, bioactivities, and electrochemistry properties of four diverse complexes with a new pyrazole ligand. Journal of Coordination Chemistry, 2010, 63, 263-272.	2.2	11
60	Five new cobalt(II) complexes based on indazole derivatives: synthesis, DNA binding and molecular docking study. Journal of Coordination Chemistry, 2019, 72, 645-663.	2.2	11
61	Synthesis and growth thermodynamic studies of CdS nanocrystals using isothermal titration calorimetry. Thermochimica Acta, 2010, 503-504, 136-140.	2.7	9
62	Room-temperature Preparation of BaMoO4 Nano-octahedra by Microemulsion Method. Chemistry Letters, 2009, 38, 404-405.	1.3	8
63	Controlled synthesis and growth mechanism of alpha nickel molybate microhombohedron. Materials Letters, 2010, 64, 695-697.	2.6	8
64	On-site generated metal organic framework-deriving core/shell ZnCo ₂ O ₄ /ZnO nanoarray for better water oxidation. Nanotechnology, 2019, 30, 495405.	2.6	8
65	Flower-like titanium dioxide as novel co-reaction accelerator for ultrasensitive "off–on― electrochemiluminescence aptasensor construction based on 2D g-C3N4 layer for thrombin detection. Journal of Solid State Electrochemistry, 2022, 26, 959-971.	2.5	8
66	Synthesis and crystal structures of supramolecular compounds: [Cu(mpca) ₂ (H ₂ O)] · 3H ₂ O and [Cu ₂ (mpca) ₂ (pyr) ₄]. Journal of Coordination Chemistry, 2009, 62, 3613-3620.	2.2	7
67	Room-temperature synthesis of MnMoO ₄ ·H ₂ O nanorods by the microemulsion-based method and its photocatalytic performance. Journal of Physics: Conference Series, 2009, 188, 012056.	0.4	7
68	Modulating the regioselectivity of solid-state photodimerization in coordination polymer crystals. Dalton Transactions, 2020, 49, 10858-10865.	3.3	7
69	Room-temperature Synthesis of CdMoO4 Nanooctahedra in the Hemline Length of 30 nm. Chemistry Letters, 2010, 39, 760-761.	1.3	6
70	Synthesis, crystal structure and properties of Zn(II) and Cd(II) complexes with 2-(4-isopropyl-4-methyl-5-oxo-4,5-dihydro-1H-imidazol-2-yl)nicotinic acid ligand. Inorganic Chemistry Communication, 2010, 13, 33-36.	3.9	6
71	Application of nBu2Sn(acac)2 for the deposition of nanocrystallite SnO2 films: Nucleation, growth and physical properties. Journal of Alloys and Compounds, 2011, 509, 7798-7802.	5.5	6
72	Homocoupling of arylboronic acids catalyzed by dinuclear copper(I) complexes under mild conditions. Journal of the Iranian Chemical Society, 2019, 16, 2639-2646.	2.2	6

#	Article	IF	CITATIONS
73	Synthesis, structure and properties of a new copper (II) complex, [Cu2(4,4′-bpy)5(H2O)4](ClO4)4(4,4′-bpy)(DMF)2(H2O)2. Inorganic Chemistry Communication, 2010, 13, 720-723.	3.9	5
74	A "Superaerophobic―Se-Doped CoS2 Porous Nanowires Array for Cost-Saving Hydrogen Evolution. Catalysts, 2021, 11, 169.	3.5	5
75	Amino group decorated coordination polymers for enhanced detection of folic acid. Spectrochimica Acta - Part A: Molecular and Biomolecular Spectroscopy, 2020, 238, 118443.	3.9	4
76	Tunable photosalient behaviours within coordination polymers <i>via</i> functional molecular prearrangements. Chemical Communications, 2022, 58, 2674-2677.	4.1	4
77	In situ Microcalorimetry Insight into the Growth of CaMoO ₄ Microcrystallites. Wuli Huaxue Xuebao/ Acta Physico - Chimica Sinica, 2009, 25, 2422-2426.	4.9	2
78	New structurally diverse photoactive cadmium coordination polymers. Dalton Transactions, 2021, 50, 18194-18201.	3.3	1
79	Nanostructure Arrays: Designing Heterogeneous 1D Nanostructure Arrays Based on AAO Templates for Energy Applications (Small 28/2015). Small, 2015, 11, 3407-3407.	10.0	0
80	Diaqua(5-methyl-1H-pyrazole-3-carboxylato)(4-nitrobenzoato)copper(II). Acta Crystallographica Section E: Structure Reports Online, 2009, 65, m210-m210.	0.2	0